

Competing Laughlin state and Wigner crystal in Bernal bilayer grapheneNgoc Duc Le  and Thierry Jolicoeur *Université Paris-Saclay, CNRS, CEA, Institut de Physique Théorique, 91190 France*

(Received 19 October 2022; revised 8 March 2023; accepted 8 March 2023; published 13 March 2023)

We study the fractional quantum Hall effect in the central Landau level of AB stacked (Bernal) bilayer graphene. By tuning the external applied magnetic field and the electric bias between the two layers one can access a regime where there is a degeneracy between Landau levels with orbital characters corresponding to $N = 0$ and $N = 1$ Galilean-Landau levels. While the Laughlin state is generically the ground state for filling $\nu = 1/3$ we find that it can be destroyed and replaced by a Wigner crystal at the same filling factor by tuning the bias and applied field. This competition does not take place at $\nu = 2/3$ where the incompressible ground state remains stable. The possibility of electrically inducing the Wigner crystal state opens a new range of studies of this state of matter.

DOI: [10.1103/PhysRevB.107.125129](https://doi.org/10.1103/PhysRevB.107.125129)**I. INTRODUCTION**

Graphene-based samples have revealed an abundance of correlated phases in the quantum Hall regime [1–16]. Odd and even-denominator fractional quantum Hall states are observed in monolayer graphene as well as in bilayer graphene and fractional Chern insulators have been realized in samples involving graphene-hexagonal boron nitride structures. Also of interest is the field-induced excitonic condensate in double-bilayer samples. It has been pointed out that AB stacked (Bernal) bilayer graphene (BLG) systems have a convenient parameter which can be tuned experimentally: the interlayer electric bias in addition to electronic density and external applied magnetic field. The central Landau level of BLG has a nearly eightfold degeneracy due to the combination of several quantum numbers: the ordinary spin, the valley degree of freedom, and also an orbital degeneracy. The pattern of ordering in these levels is then very rich and complex. It has been shown that there are tunable phase transitions in fractional quantum Hall states [17]. The electric bias directly controls the splitting between orbital levels and the Coulomb interaction between electrons is also impacted by the value of the external applied magnetic field as well as the bias. Detailed investigations of the integer quantum Hall states have been performed on these systems [18] and have shown that an appropriate tight-binding model can capture the level ordering. Recent advances have led to the observation of many fractional states and transitions between them. This means that we have at our disposal a physical system where we can tune parameters affecting the fractional quantum Hall physics [19–27].

In the case of two-dimensional electron systems in GaAs it is known that there is a competition between incompressible electron liquids and crystal of electrons, the so-called Wigner crystal. For filling factor $\nu = 1/3$ of the lowest Landau level, the ground state of the electronic system with Coulomb interactions is an incompressible liquid whose properties are well described by the Laughlin wave function [28] and it is only for small filling factors that the ground state is a crystal state [29]. Deciding the precise boundary between these phases has proven a difficult issue [30]. The crystal state appears as an

insulating state with a diverging longitudinal resistance when decreasing the temperature. There are experimental evidences for reentrance of the Wigner crystal when one decreases the filling factor. Studies of the crystal state are difficult due to the large values of the magnetic field needed to destroy the fractional quantum Hall liquids. The crystal state is not the only competitor with the liquid states. In higher Landau levels it is known that the electronic system may also form the so-called stripe or bubble phases. As the Wigner crystal such states break translation symmetry and it is believed that they are in a distinct state of matter without topological order. Their experimental signature is an insulating behavior with additional anisotropic properties. We note that in two-dimensional GaAs electron or hole systems [31–35] there is a rich competition between several many-body ground states and that the Wigner crystal can be stabilized at or close to filling $1/3$ by tuning gate potentials.

Graphene systems offer yet another arena for the study of such competing phases, in particular the AB stacked bilayer graphene due to its tunability. It is also known that mixing with higher Landau levels can bias the competition towards the Wigner crystal state. Tuning the BLG system to obtain degeneracy of Landau levels with $N = 0$ and $N = 1$ character can be viewed as an extreme example of Landau level mixing albeit with the absence of levels with $N > 1$. So it is plausible that the competition between the Laughlin state and the Wigner crystal can be tuned.

In this paper we investigate the incompressible quantum Hall states that occur for filling factor $\nu = 1/3$ and $\nu = 2/3$ when the system is fully valley as well as spin polarized in the AB stacked bilayer graphene system. The interesting physics now emerges from the crossing of levels with orbital character $N = 0$ and $N = 1$. This should happen in the central octet of Landau levels for fillings close to $\nu = -3$ according to the present knowledge of level orderings [24]. Electrons form then an effective two-component system with a tunable anisotropic interaction given by the projection of the Coulomb potential into this two-component subspace. We use the exact diagonalization technique in the torus geometry which is well suited to study the competition

between incompressible quantum Hall phases and the Wigner crystal [36–39].

For the filling factor $\nu = 1/3$ we find that the Laughlin-like ground state is stable in a wide region of the phase diagram of the BLG system. However there is a region enclosing the degeneracy point where it is no longer the ground state. We observe the appearance of a set of quasidegenerate ground states that form a lattice in reciprocal space as expected for spontaneous breakdown of translational symmetry. The crystalline correlations are also revealed by computing an appropriate pair correlation function. The crystal state is fully polarized in the $N = 0$ orbitals since the exchange energy is larger than in the $N = 1$ case. It appears close to the boundary of a polarization transition. The transition to the Laughlin state is either second order or weakly first order since the the ground state manifold includes a zero-momentum state that smooth deforms into the Laughlin state.

In the case of the fraction $\nu = 2/3$ we find no such crystal state but only a smooth crossover between the fully spin polarized state which is the particle-hole transform of the $\nu = 1/3$ state and the singlet state.

In Sec. II we describe the consequences of the band structure of AB stacked bilayer graphene onto the Landau levels and discuss the effective Hamiltonian we use. Section III discusses our findings about the Laughlin state and the Wigner crystal. Section IV is devoted to the fraction $\nu = 2/3$ where incompressible liquids are always stable. Finally, Sec. V presents our conclusions.

II. QUANTUM HALL EFFECT IN AB STACKED BILAYER GRAPHENE

Monolayer graphene has a well-known peculiar band structure with two bands touching by Dirac cones at two different wave vectors in the Brillouin zone, leading to two valleys. A closely related material is the AB stacked bilayer graphene also called Bernal stacking. The unit cell has now four atoms due to the additional layer and we have four bands capturing the low-energy properties. These bands still touch in two points of the Brillouin zone but with a quadratic band touching. It is possible to apply an electric field perpendicular to such a sample and to open a band gap that is tunable experimentally. If now we apply a perpendicular magnetic field we create a peculiar Landau level structure. At zero energy we find a set of approximately eightfold degenerate Landau levels. This degeneracy comes from the usual spin degeneracy with index $\sigma = \uparrow, \downarrow$. As in monolayer graphene there is a valley twofold degeneracy with indices $\tau = K, K'$. There is also a degeneracy between levels with different orbital characters which is unique to the bilayer system.

We denote the wave functions [40,41] of these states as $\psi_{N\sigma\tau}$ with $N = 0, 1$. A four-band calculation with appropriate microscopic parameters gives the necessary input for our studies. The $\psi_{1\sigma\tau}$ wave functions have weight concentrated onto the $n = 0$ and $n = 1$ cyclotron Galilean orbitals that we denote by $\phi_{0,1}$:

$$\psi_{1K\uparrow} = (\sqrt{1-\gamma}\phi_1, 0, \gamma\phi_0, 0), \quad (1)$$

$$\psi_{1K'\uparrow} = (0, \sqrt{1-\gamma}\phi_1, 0, \gamma\phi_0), \quad (2)$$

where the four components denote amplitudes on the four sites A, B', A', B of the BLG unit cell. The sites are defined as in Ref. [40]. In what follows the integer index N stands for BLG orbitals while n refers to Galilean orbitals deriving from electrons with a parabolic dispersion relation. Similarly we have

$$\psi_{0K\uparrow} = (\phi_0, 0, 0, 0), \quad (3)$$

$$\psi_{0K'\uparrow} = (0, \phi_0, 0, 0). \quad (4)$$

These formulas for the Landau level wave functions comes from a detailed band structure calculation. We have omitted the ever present Landau degeneracy of each level which is equal to the number of flux quanta though the sample. The γ parameter can be adjusted by the external magnetic field and has an almost linear variation from $\gamma = 0.01$ for $B = 2T$ to $\gamma = 0.35$ at $B = 45T$ according to Ref. [18]. This parameter also varies with the electric bias u between the layers.

In this work we concentrate on the case of spin and valley polarized fractional quantum Hall states but we study the influence of the possible degeneracy of $N = 0$ and $N = 1$ states. We thus project the Coulomb interaction onto this two-component subspace. So we make the approximation of neglecting the mixing to higher Landau levels, necessary to reduce the Fock space dimension to a manageable size. This will be accurate only in a small region of available parameter space. However this allows us to explore the situation of orbital degeneracy unique to the BLG system.

Coulomb interactions are isotropic in spin and valley space to a very good approximation but there is no good symmetry between the two orbital states since the matrix elements of the interaction are very different between the two $n = 0$ and $n = 1$ Landau levels. The second-quantized Hamiltonian can be written as

$$\mathcal{H} = \frac{1}{2A} \sum_{q\{N_i\}} \tilde{V}(q) F_{N_1 N_2}(q) F_{N_3 N_4}(-q) \cdot \rho_{N_1 N_2}^\dagger(q) \rho_{N_3 N_4}(q) + \Delta_{10} \hat{N}_0. \quad (5)$$

The operators $\rho_{nm}(q)$ are projected density operators with the following form factors:

$$F_{00} = e^{-q^2/4}, \quad F_{11} = ((1-\gamma)L_1(q^2) + \gamma L_0(q^2))e^{-q^2/4}, \\ F_{10} = F_{01}^* = \sqrt{1-\gamma} \frac{q_y - iq_x}{\sqrt{2}} e^{-q^2/4}. \quad (6)$$

Here we use the Coulomb potential $\tilde{V}(q) = 2\pi e^2/\epsilon|q|$, A is the area of the system. L_0 and L_1 are Legendre polynomials. Strictly speaking the Coulomb interactions between electrons in different layers is suppressed by a factor e^{-qd} where d is the distance between layers. In the case of BLG in the quantum Hall regime d is always much smaller than the magnetic length $\ell = \sqrt{\hbar/eB}$ so that $d/\ell \ll 1$. We neglect this small correction in this work and set $d = 0$. In BLG systems the screening effects may modify the Coulomb potential. We have used the modification proposed in Ref. [42] and checked that our results do not depend sensitively upon screening effects

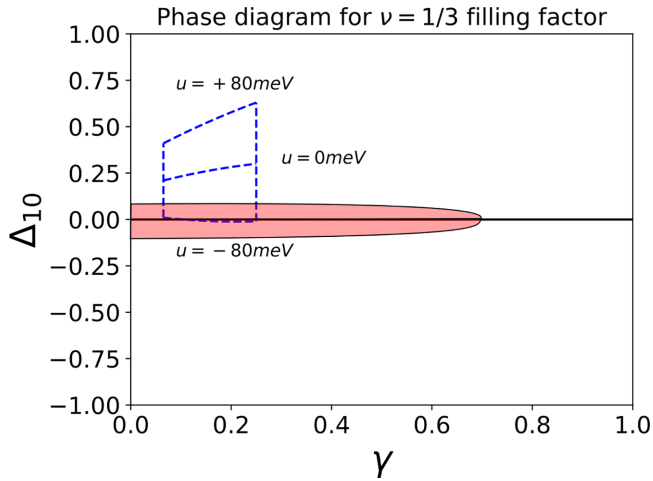


FIG. 1. The phase diagram at filling factor $\nu = 1/3$ in the $\gamma = 0$ and Δ_{10} plane. In the lower part corresponding to Δ_{10} negative one recover the lowest Galilean-Landau level physics of the Laughlin-like $\nu = 1/3$ incompressible state. In the upper part it is the second Landau level physics which is recovered with presumably an incompressible state in the same universality class as the Laughlin state. The right boundary of the diagram with $\gamma = 1$ is a spinfull system of electrons with the LLL form factor. The nontrivial region is the neighborhood of the $\gamma = 0$ and $\Delta_{10} = 0$ with full mixing of the two orbitally distinct Landau levels of BLG. In the red region we find that the Laughlin state is replaced by a Wigner crystal of electrons with a triangular structure. Its extension goes up to $\gamma \approx 0.7$ and it is located in a narrow range of orbital splitting of at most $\Delta_{10} \in [-0.08, +0.06]$ for $\gamma = 0$. In devices based on BLG samples [8,18,24] typical values of γ , Δ_{10} are given by the three curves with interlayer bias $u = -80, 0, +80$ meV for magnetic field varying between $B = 10T$ on the left-hand side (vertical blue dotted line at $\gamma = 0.06$) and $B = 45T$ on the right (vertical blue line at $\gamma = 0.25$). The Wigner crystal transition can be reached for realistic field strengths with negative enough bias.

as was observed previously [43]. So the results presented in this paper are for the bare Coulomb potential. We measure all lengths in units of the magnetic length $\ell = \sqrt{\hbar/eB}$ and energies are measured via the Coulomb scale $e^2/(\epsilon\ell)$. We explore the fractional quantum Hall effect (FQHE) phase diagram as a function of the γ parameter which has a range $[0, 1]$ and also as a function of the level splitting Δ_{10} . So the two theoretical parameters are controlled by u and B : $\gamma \equiv \gamma(u, B)$ and $\Delta_{10} \equiv \Delta_{10}(u, B)$. While strictly speaking the range of the Δ_{10} parameter is unbounded, all interesting variations occur if we vary it in the interval $\Delta_{10} = +1 \cdots -1$ in units of the Coulomb energy scale. In bilayer graphene the splitting Δ_{10} is controlled mostly by the interlayer bias u . The precise relation has been explored in some details [18]. At zero bias $u = 0$ there is nevertheless a nonzero splitting of $N = 0$ and $N = 1$ states due to the Lamb shift-like effect of the Fermi sea of all filled levels below the central octet. Achieving degeneracy $\Delta_{10} = 0$ requires tuning u to negative values in the conventions of Ref. [18]. In Fig. 1 we have plotted three lines giving the values of γ and Δ_{10} when we vary the magnetic field at fixed interlayer bias $u = +80, 0, -80$ meV.

Several limiting cases can be reached as a function of these parameters. When $\gamma = 1$ the Coulomb interaction is identical

to that of the lowest Landau level of nonrelativistic electrons irrespective of the orbital index since then we have $F_{00} = F_{11}$ and there are no Coulomb couplings between the orbitals $F_{10} = F_{01} = 0$. So there is complete $SU(2)$ symmetry in the $n = 0, 1$ space and the problem is formally equivalent to a Galilean lowest Landau level system with spin and zero Zeeman energy if $\Delta_{10} = 0$. Varying Δ_{10} at $\gamma = 1$ is exactly like applying a Zeeman energy on the $SU(2)$ symmetric Coulomb interacting lowest Landau level. So we recover the physics of the FQHE in the lowest Landau level with two components. Many fractions are known to be present in this limiting case and their properties are mostly understood [44] at least for $\nu = 1/3$ and $\nu = 2/3$ most prominent cases.

If now we set γ to zero we have two orbitals with the form factors of the lowest $n = 0$ and second $n = 1$ Landau levels whose degeneracy is controlled again by Δ_{10} . For Δ_{10} large and negative we are back to a single polarized lowest Landau level (LLL) while for Δ_{10} large and positive the physics is that of a single polarized *second* Landau level. If $\Delta_{10} = 0$ we have maximal mixing between the two degenerate $n = 0$ and $n = 1$ orbitals, a situation unique to bilayer graphene. This is a situation which is reminiscent of strong Landau level mixing. Indeed when the cyclotron energy is not very large with respect to the Coulomb energy scale virtual transitions towards empty levels will modify the interactions between electrons residing in the LLL. This effect in general destabilizes the FQHE states [48] and favors the appearance of the Wigner crystal state as is the case for example in two-dimensional hole systems [35] So the two-component system at $\gamma = 0$ can possibly share some of the physics of Landau level mixing with the caveat that higher-lying Landau levels are missing in the BLG system (strictly speaking they are at much higher energies).

When Δ_{10} is very large and negative all electrons stay in the $N = 0$ orbitals and the presence of the $N = 1$ orbitals is manifest only through virtual interactions. This effect vanishes for very large Δ_{10} which means that the γ parameter no longer plays any role. One observes then the physics of fully polarized electrons with the standard bare Coulomb interactions in the lowest Galilean-Landau level. For Δ_{10} is very large and positive and all electrons are now in the $N = 1$ levels with a γ -dependent interaction as given by F_{11} . This is a fully polarized situation which interpolates between the lowest Landau level interaction for $\gamma = 1$ and the $n = 1$ Landau level interaction for $\gamma = 0$. This last case is also known to harbor quantum Hall liquids but with the added complication of competing phases. We note that for $\gamma = 1/2$ the interaction is exactly the one which is relevant for the $N = 1$ Landau level of monolayer graphene.

To make progress we perform exact diagonalizations of the many-body problem defined by Eq. (5) in a $L_x \times L_y$ rectangular unit cell with periodic boundary conditions. The total number of flux quanta through this system is quantized to an integer value $N_\phi = L_x L_y / 2\pi$. Such a finite area leads to a finite dimensional Fock space without any *ad hoc* truncation. Exact diagonalizations have proved to be an invaluable tool for nonperturbative exploration of fractional quantum Hall physics. This unit cell has an adjustable parameter called the aspect ratio $AR = L_x/L_y$. The periodic boundary conditions are imposed on this unit cell and we construct the many-body

translation operators that are used to classify the eigenstates [36,45]. The corresponding eigenvalues are $K_x = 2\pi s/L_x$, $K_y = 2\pi t/L_y$, where s and t are integers varying in the interval $0, \dots, N$, where N is the greatest common denominator of N_e and N_ϕ . The origin of the quantum numbers s, t is not always zero. When $pq(N_e - 1) = 2k + 1$ for $\nu = p/q$ (p, q coprime) the zero momentum state is located at $s_0 = t_0 = N/2$, otherwise it is located at $s = t = 0$. This shift is of no special physical significance. Previous studies [43,46,47] for fillings $\nu = 1$ and $\nu = 1/2$ have revealed a rich physics. Indeed for $\nu = 1$ a case where we expect an instance of quantum Hall ferromagnetism, there is evidence for an helical phase. In the case $\nu = 1/2$ there is a complex competition between the Moore-read paired state and the Fermi sea of composite fermions with possible appearance of an exotic anisotropic gapless phase. In what follows we mainly explore the fate of the celebrated fraction $\nu = 1/3$ well known in semiconductor devices as well as graphene systems.

III. THE FATE OF THE LAUGHLIN STATE $\nu = 1/3$

We now focus onto the most prominent fraction $\nu = 1/3$ and study its stability in the $\Delta_{10} - \gamma$ phase diagram. With the limiting values for γ and Δ_{10} the phase diagram can be drawn in a rectangle, see Fig. 1.

Along the $\gamma = 1$ line, which is the vertical rightmost boundary, the two orbitals have exactly the same form factor and there is no mixing between them since we have $F_{10} = F_{01} = 0$. The external field Δ_{10} is exactly analogous to a Zeeman field and the Coulomb interaction has the $SU(2)$ symmetry between the two components. At filling factor $\nu = 1/3$ we should thus find the incompressible Coulomb FQHE state well approximated by the Laughlin wave function [28]. This FQHE state is fully polarized for Δ_{10} large, be it positive or negative. For the degeneracy point $\Delta_{10} = 0$ we have an unbroken $SU(2)$ symmetry and it is known that we have then an instance of quantum Hall ferromagnetism: the Laughlin state is a multiplet with total spin $S_{\text{tot}} = N_e/2$ where ‘‘spin’’ refers to the two components $N = 0/1$. Adding a nonzero Zeeman-like energy will lift completely the degeneracy of the ground state multiplet favoring the $S_{\text{tot}}^z = +N_e/2$ or $-N_e/2$ according to the sign of Δ_{10} .

Along the $\Delta_{10} = -1$ line the system becomes one-component and the Coulomb interaction is governed by the form factor F_{00} which is independent of γ . So we recover the lowest Landau physics of the $\nu = 1/3$ Laughlin-like state.

If we now explore the $\Delta_{10} = +1$ boundary the system is also one-component but interactions are ruled now by the form factor F_{11} which is γ dependent. For $\gamma = 1$ the interaction is exactly that of the Galilean LLL while for $\gamma = 0$ it is the interaction of the *second* Landau level. In between we observe that the value $\gamma = 1/2$ gives the form factor appropriate to the $N = 1$ Landau level of monolayer graphene. We are not able to shed any new light on the nature of the $\nu = 1/3$ state in the second Landau level. It is known that finite size effects become important and that a finite width of the electron gas is necessary to stabilize the Laughlin state. Here we take the simple view that the Laughlin state is still a valid description of $\nu = 1/3$ even in this case. As a consequence the set of boundaries (large negative Δ_{10} , any γ), (any

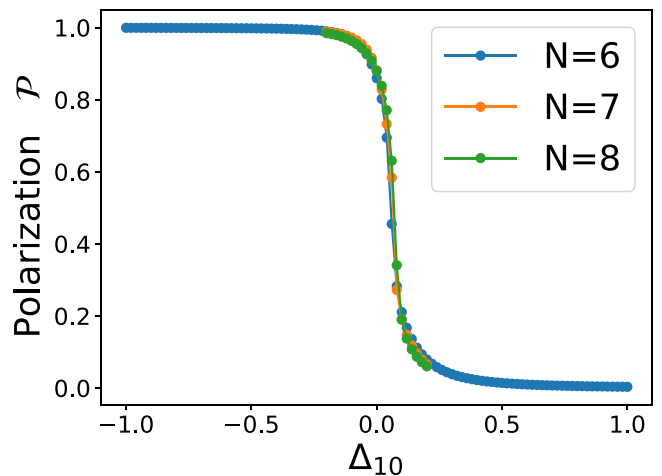


FIG. 2. The polarization of the zero-momentum ground state at $\nu = 1/3$ for $\gamma = 0$ as a function of Δ_{10} . The curve is very weakly dependent upon the aspect ratio of the unit cell. For large negative values all electrons prefer to occupy the $N = 0$ orbital while for large positive Δ_{10} they occupy the $N = 1$ orbitals. We note that the transition between these two regimes happens for a nontrivial value of the bare splitting $\Delta_{10} \approx 0.06$ insensitive to the system sizes we have studied. Sizes are $N_e = 6, 7, 8$ electrons.

$\Delta_{10}, \gamma = 1$), (large positive Δ_{10} , any γ) all share the same Laughlin-like physics differing only by polarization. So the most interesting region is the small γ small Δ_{10} region. We expect that varying Δ_{10} will induce a polarization transition between the two components. So to locate phase boundaries we use two indicators: the polarization of the ground state and the quantum fidelity.

A. Polarization transition

It is natural to define a polarization of the two-component system of any quantum state Ψ by the following quantity:

$$\mathcal{P} = \langle \Psi | \hat{N}_0 | \Psi \rangle / N_e, \quad (7)$$

that will track the orbital content of the state under consideration. With the normalization we have chosen $\mathcal{P} = 1$, which corresponds to all electrons residing in the $N = 0$ orbital. We infer that for any state \mathcal{P} will vary from $+1$ in the lower part of the phase diagram for Δ_{10} negative to zero in the upper part for Δ_{10} positive. Exactly on the $\gamma = 1$ line the behavior of \mathcal{P} can be inferred from the nature of the spin multiplet of the ferromagnetic Laughlin state. The curve is a simple staircase with two values according to the discussion about the quantum Hall ferromagnetism above. For $\gamma < 1$ the curve is nontrivial. We find that the polarization curve is now rounded and has a sharp decrease when Δ_{10} goes up in all parts of the phase diagram. However, the inflection point of the curve is no longer pinned at $\Delta_{10} = 0$ but is at positive nonzero values for small enough γ . We display in Fig. 2 the case of $\gamma = 0$ which is the leftmost boundary of the phase diagram. We find that the sharp transition happens for $\Delta_{10} \approx 0.06$ almost independently of the size of the system. When γ is nonzero the sharp transition happens for decreasing values of Δ_{10} . A

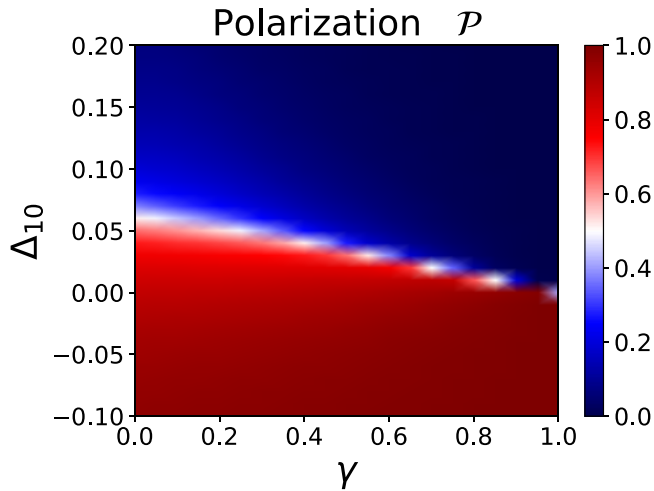


FIG. 3. Polarization of the zero-momentum ground state for $N=6$ electrons as a function of the γ parameter and the splitting Δ_{10} between the two levels. In the $SU(2)$ symmetric case for $\gamma = 1$ the transition happens right at $\Delta_{10} = 0$ while it is shifted in the upper half plane when $\gamma < 1$.

map of the polarization is given in Fig. 3. This is expected since the exchange energy is stronger in the LLL with respect to the second Landau level. So even when $\Delta_{10} = 0$ it is more favorable energetically to polarize the system in the lowest Landau level. One needs a finite amount of offset energy Δ_{10} to overcome the exchange energy gain.

In the complete phase diagram we find a phase boundary given in Fig. 3 where we see the polarization boundary evolving smoothly.

B. Using fidelity to locate phase boundaries

To locate phase boundaries one can also compute overlaps of different ground states obtained by changing a parameter of the Hamiltonian. An infinitesimal version of the overlap calculation is the so-called quantum fidelity:

$$\mathcal{F}(\delta) = |\langle \Psi(\delta + \epsilon) | \Psi(\delta) \rangle|, \quad (8)$$

where δ is the parameter we choose to vary and ϵ an infinitesimal increment. Phase transitions are expected to appear as a strong dip away from unity and the bigger the size the stronger the dip. We have computed the fidelity across the phase diagram and it is sensitive to the polarization transition that we observed above. A sample behavior at fixed γ as a function of Δ_{10} is given in Fig. 4. The characteristic dip grows with the size of the system as expected for a phase transition. With only these two indicators there is no sign of other phase boundaries.

C. The Wigner crystal

Beyond the simple two-phase picture given by the polarization and fidelity transition of the section above we nevertheless find that the physics changes drastically in the region of small γ and small Δ_{10} . Indeed we observe the appearance in the spectrum of a set of nearly-degenerate low-energy states well separated from higher-energy states by a

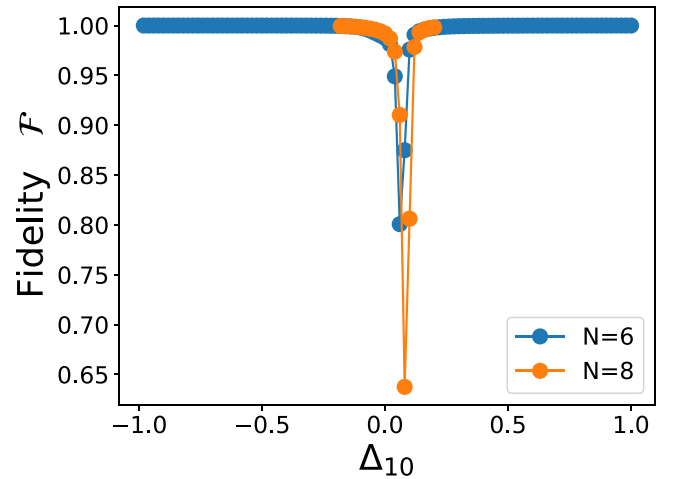


FIG. 4. The fidelity at $\nu = 1/3$ for $\gamma = 0$ as a function of Δ_{10} . We track the zero-momentum ground state. There is evidence that for a transition between two regimes happens for a nontrivial value of the bare splitting $\Delta_{10} \approx 0.06$ weakly sensitive to the system sizes we have studied. This is numerically equal or very close to the value of maximal slope of the polarization curve.

gap. We call these states the ground state manifold. One has to fine tune the aspect ratio of the periodic unit cell used in the diagonalization [36–38] to obtain the degeneracy. This is a typical occurrence of broken symmetry in a finite system. This phenomenon has been observed in the lowest Galilean-Landau level for small filling factors and is an evidence of a Wigner crystal ground state as found in Refs. [36–38]. An example is displayed in the right panel of Fig. 5 where the energy eigenvalues are plotted as a function of the momentum. The set of almost degenerate states has an energy splitting of the order of at most $\approx 10^{-4}$ in Coulomb scale units as opposed to excitation energies of $O(10^{-2})$. If plotted in the Brillouin zone the momenta of the quasidegenerate states display a regular lattice which is the reciprocal lattice of a crystal structure as seen in the right panel of Fig. 5. In most cases we have studied the lattice is almost triangular. Also the number of states in the quasidegenerate manifold is equal to the number of electrons, ruling out bubble or charge density wave states [36–38].

This manifold of states is sensitive to the aspect ratio L_x/L_y of the unit cell in which we diagonalize the Hamiltonian. There is an optimal value which is size dependent as is the case of the low-filling factor Wigner crystal: $L_x/L_y = 0.44$ for $N_e = 6$, 0.37 for $N_e = 7$, 0.7 for $N_e = 8$, 0.3 for $N_e = 9$. From observation of spectra like the ones presented in Fig. 6 it is difficult to pinpoint a phase boundary separating the Wigner crystal from the Laughlin state. We just observe a crossover with no striking discontinuity or (obvious) nonanalyticity. An example of the crossover is given in Fig. 6. For positive splitting Δ_{10} the crystal does not survive the polarization transition and the degeneracy is destroyed. If we increase γ we also find that the crystal signature disappears close to $\gamma \approx 0.7$.

To characterize the crystalline order we also compute the pair correlation function:

$$g_{\alpha\beta}(R) = \frac{1}{\rho N_e} \sum_{i \neq j} \delta(r_i - r_j - R) |\langle \alpha | \langle \alpha | \rangle| |\langle \beta | \langle \beta | \rangle|, \quad (9)$$

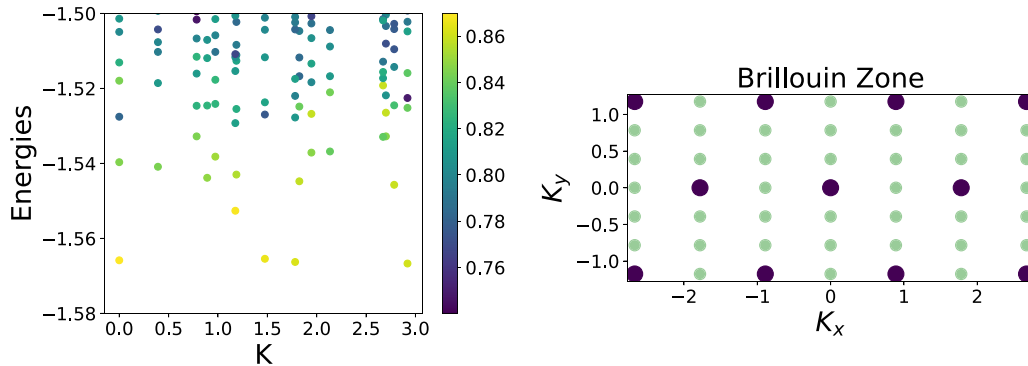


FIG. 5. Energy spectrum for six electrons with $\gamma = 0$ and exact degeneracy $\Delta_{10} = 0$. The energies are plotted as a function of the momentum K in a rectangular cell of aspect ratio 0.44. The color indicates the polarization of the low-lying eigenstates. There is a set of quasidegenerate states clearly separated from the remainder of the spectrum. They are all essentially fully polarized in the $N = 0$ orbital subspace.

where $\alpha, \beta = 0, 1$ is the orbital index and electron coordinates are r_i, r_j , ρ is the density. In this definition the pair correlation is periodic $g_{\alpha\beta}(x + L_x, y) = g_{\alpha\beta}(x, y)$, $g_{\alpha\beta}(x, y + L_y) = g_{\alpha\beta}(x, y)$. The almost full polarization of the crystal states means that only g_{00} is sizable. Indeed we find that other components g_{11}, g_{10}, g_{01} track the pattern seen in g_{00} . In the region of degeneracies we observe directly a crystal structure in real space from g_{00} as displayed in Fig. 7. A liquid state has instead a single crater-like feature around the position of the reference particle and a smooth background beyond a first ring of overdensity. Here what we observe is definitely a state modulated in real space and the lattice of electrons has the reciprocal lattice we observe in the manifold of degenerate states. We take this as evidence for a crystal state. The number of overdensities plus the central electron is equal to the total number of electrons, again consistent with a Wigner crystal. The case of $N_e = 8$ is special: the lattice formed is square as can be seen in the central panel of Fig. 7 and the momenta in

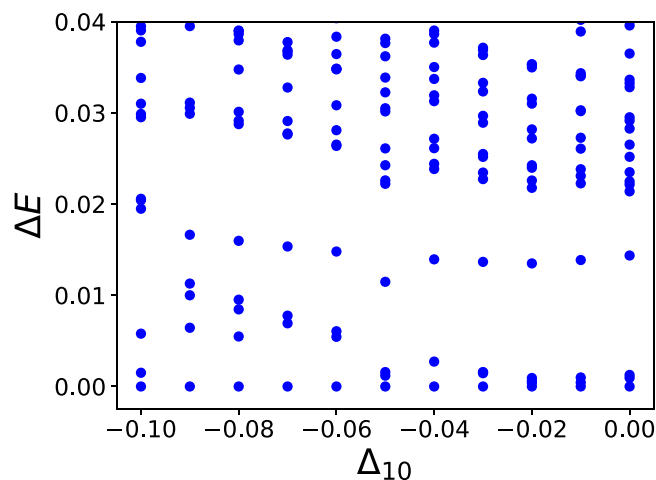


FIG. 6. Excitation energies above the ground state as a function of Δ_{10} for $\gamma = 0$ for a system of $N_e = 6$ particles at $\nu = 1/3$ in a rectangular unit cell of aspect ratio $L_x/L_y = 0.44$. When there is orbital degeneracy $\Delta_{10} = 0$ we observe a set of quasidegenerate states pointing to broken translational symmetry. An increase of the pseudo-Zeeman field lifts the degeneracies in a smooth crossover starting around $\Delta_{10} \approx -0.02$.

the Brillouin zone also form a square lattice. While we cannot ultimately conclude on the precise nature of the lattice, this is indicative of a close competition between triangular and square lattices.

To characterize the crystal strength we can measure the contrast around the first ring of overdensity in the pair correlation function which is prominent both in solid and liquid phases. In the crystal state we find a contrast $(g_{\max} - g_{\min})/g_{\min} \approx 0.44$ when $\gamma = 0$ and $\Delta_{10} = 0$ for $N_e = 9$. If we consider the liquid Laughlin state the contrast is only 0.07 for a system of the same size. The Coulomb ground state at $\nu = 1/3$ in a single polarized Landau level, well described by the Laughlin state, has even less contrast ≈ 0.04 . We use this quantity to pin down the boundary of the crystal phase in the region with negative Δ_{10} . We decide quite arbitrarily that the state is liquid when the contrast is less than 0.1. This gives a rough estimate of the stability region, leading to the red island in Fig. 1. As a comparison we display in Fig. 8 the pair correlation for one-component spin-polarized electrons in the lowest Galilean-Landau level for $N_e = 8$ electrons at filling factor $\nu = 1/7$ where we expect a Wigner crystal [36]. Indeed the contrast is now close to 2 along the ring circling the reference electron at $r = 0$. We attribute this difference to the fact that the unit cell is now larger in real space for the fraction $\nu = 1/7$: this case has $N_\phi = 56$ leading to sizes $L_x = 11.9$ and $L_y = 29.6$ while our largest system for $N_e = 9$ has $L_x = 7.1$ and $L_y = 23.8$ so finite size effects are presumably stronger for the bilayer case.

Finally, we note that the Wigner state appears to be almost fully polarized: See the color bar in Fig. 5 as a representative example. An interesting question is whether this state is totally polarized $\mathcal{P} = 1$ or almost fully polarized $\mathcal{P} \lesssim 1$. From our numerical measurements we cannot discriminate between these two possibilities. With the accessible sizes finite size scaling is not conclusive. Partial polarization would be an interesting new phenomenon. Nontrivial modifications of existing trial wave functions would be required to explain such a state.

IV. BEHAVIOR OF THE $\nu = 2/3$ STATE

We now turn to the study of the FQHE state at filling factor $\nu = 2/3$. Due to the two-component nature of the BLG

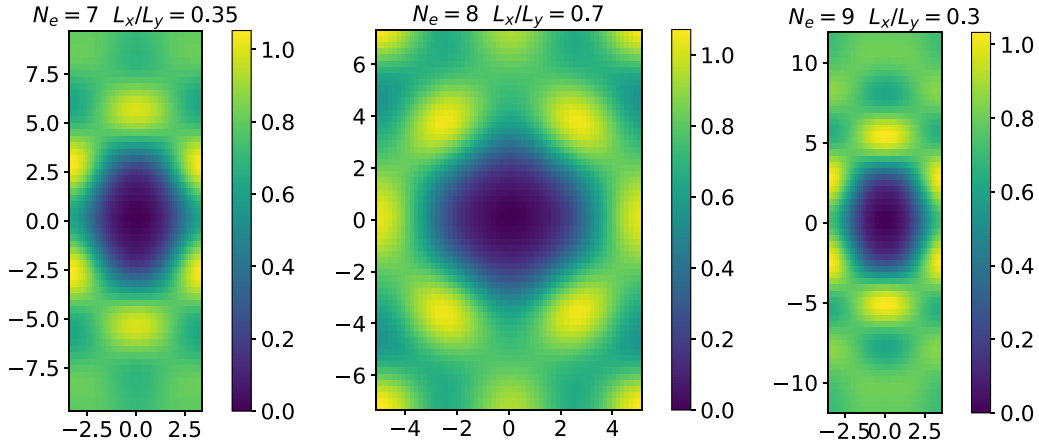


FIG. 7. The pair correlation function $g_{00}(x, y)$ for $N_e = 7$ (left), $N_e = 8$ (center), $N_e = 9$ (right) electrons at $\nu = 1/3$ for $\Delta_{10} = 0$ and $\gamma = 0$. The electron located at the origin gives a deep correlation hole in addition to the Pauli zero. The aspect ratio is chosen so as to favor the appearance of the crystal structure. This value of L_x/L_y is size dependent. For $N_e = 7, 9$ (left and right) there is evidence for a triangular crystal state while it is a square lattice that appears for $N_e = 8$ (center). We note that revealing the square case requires a different aspect ratio than for the triangular case.

states this is not simply the particle-hole conjugate of the $\nu = 1/3$ case which happens indeed at $\nu = 2 - 1/3 = 5/3$. We start by discussing the physics for $\gamma = 1$ as a function of the external field Δ_{10} . In this limiting case we have full $SU(2)$ symmetry in the orbital space only broken by the Zeeman-like field Δ_{10} . For two-component FQHE states at $\nu = 2/3$ we know that there are two incompressible candidate states that

compete. The first candidate is the particle-hole conjugate of the $\nu = 1/3$ state where the particle-hole symmetry does not involve the spin degrees of freedom. It can be viewed as a composite fermion state with negative effective flux and two filled effective Landau levels [44]. This state is fully polarized and in the absence of Zeeman energy it gives rise to an exactly degenerate ferromagnetic spin multiplet. The other candidate state is the $\nu = 2/3$ global spin singlet state which is known to be the ground state in the absence of Zeeman energy, i.e., it is definitely lower than the fully polarized $2/3$ state. For $\gamma = 1$ there is a sharp transition between these two ground states as a function of Δ_{10} by translation of the known spin physics.

If we now consider the realistic case of $\gamma < 1$, the $SU(2)$ symmetry is explicitly broken and nothing precludes a continuous transformation between these two states. This is indeed what we observe in our diagonalizations. We find no transitions in the interior region of the phase diagram. At $\gamma = 1$ and varying Δ_{10} the polarization \mathcal{P} has two sharp transitions from $+1$ to $1/2$ and then to 0 which correspond to the expected spin transitions of $\nu = 2/3$, the plateau at $\mathcal{P} = 1/2$ corresponding to the singlet state. For $\gamma < 1$ these steps are rounded and no transitions remain. We conclude that there is no Wigner crystal state at $\nu = 2/3$.

V. CONCLUSIONS

We have studied by exact diagonalization techniques in the torus geometry the fate of the quantum Hall states at $\nu = 1/3$ and $\nu = 2/3$ in the AB stacked bilayer graphene system when there is almost coincidence of Landau levels with $N = 0$ and $N = 1$ orbital character. The detailed quantitative studies of Ref. [8] have shown that this level coincidence can happen for $\nu_{BLG} = -3 + 1/3, -3 + 2/3$ notably. Previous studies of this coincidence [47] have shown a complex competition of phases for the half-filled case. By tuning the applied magnetic field and the electric bias between the layers we find that it is possible to destabilize the Laughlin incompressible state for filling $\nu = 1/3$ and create a Wigner crystal of electrons. This crystal is stabilized when the $N = 0$ and $N = 1$ are in

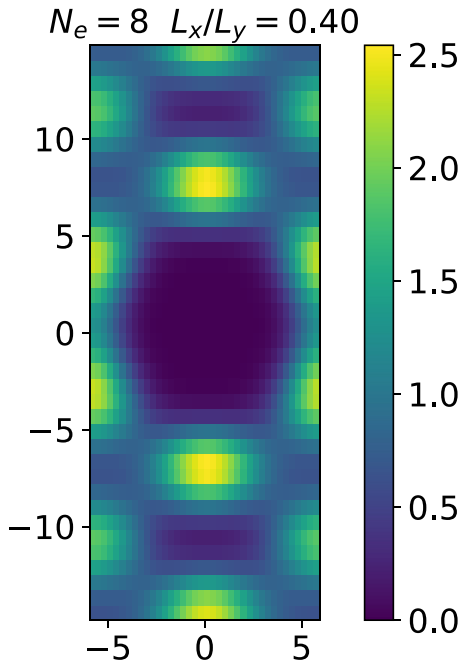


FIG. 8. The pair correlation function $g(x, y)$ for $N = 8$ electrons in the lowest Galilean-Landau level at filling factor $\nu = 1/7$. The aspect ratio is taken to be $L_x/L_y = 0.4$ to favor the appearance of the crystal structure as was observed for smaller system sizes in Refs. [36–38]. There are eight overdensities which is consistent with a Wigner crystal with one electron per site and a triangular structure. The density contrast is much higher for this system size and aspect ratio than in the case of the bilayer system.

almost coincidence creating a situation akin to extreme Landau level mixing [48] with the difference that there are no extra levels beyond $N = 1$. The crystal structure is revealed by the quasidegeneracies in the many-body spectrum as well as by the pair correlation function. The crystal is favored by fine tuning the rectangular unit cell we use in exact diagonalizations. The crystal structure seen in real space from the measurement of the pair correlation has the same reciprocal lattice as observed in the magnetic Brillouin zone for the quasidegenerate states. There is a polarization transition that coincides with the boundary of the crystal phase for positive values of Δ_{10} at least when γ is small enough. For negative values of the level splitting we use the contrast of the ring of overdensity of the pair correlation to locate the other phase boundary. The resulting map of the crystal state is given in our Fig. 1. The simplest way to observe the transition is to measure the longitudinal resistance that should have a sharp peak when there is level coincidence. Thermodynamic

measurements like the chemical potential can be used [16]. The interlayer bias should be large enough while there is no real restriction of the value of the magnetic field which controls the γ parameter. The phase transition between the crystal state and the Laughlin state involves only a smooth lifting of the degeneracy of the ground state multiplet and the zero-momentum state is always a member of the degenerate states, deforming continuously into the Laughlin state. This is compatible with a weakly first-order or second-order transition.

ACKNOWLEDGMENT

We acknowledge discussions with A. Assouline and thank M. Shayegan for useful correspondence. We thank DRF and GENCI-CCRT for computer time allocation on the Topaze cluster.

-
- [1] X. Du, I. Skachko, F. Duerr, A. Luican, and E. Y. Andrei, *Nature (London)* **462**, 192 (2009).
- [2] K. I. Bolotin, F. Ghahari, M. D. Shulman, H. L. Stormer, and P. Kim, *Nature (London)* **462**, 196 (2009).
- [3] F. Ghahari, Y. Zhao, P. Cadden-Zimansky, K. Bolotin, and P. Kim, *Phys. Rev. Lett.* **106**, 046801 (2011).
- [4] C. R. Dean, A. F. Young, P. Cadden-Zimansky, L. Wang, H. Ren, K. Watanabe, T. Taniguchi, P. Kim, J. Hone, and K. L. Shepard, *Nat. Phys.* **7**, 693 (2011).
- [5] A. F. Young, C. R. Dean, L. Wang, H. Ren, P. Cadden-Zimansky, K. Watanabe, T. Taniguchi, J. Hone, K. L. Shepard, and P. Kim, *Nat. Phys.* **8**, 550 (2012).
- [6] B. E. Feldman, B. Krauss, J. H. Smet, and A. Yacoby, *Science* **337**, 1196 (2012).
- [7] B. E. Feldman, A. J. Levin, B. Krauss, D. A. Abanin, B. I. Halperin, J. H. Smet, and A. Yacoby, *Phys. Rev. Lett.* **111**, 076802 (2013).
- [8] B. Hunt, J. D. Sanchez-Yamagishi, A. F. Young, M. Yankowitz, B. J. LeRoy, K. Watanabe, T. Taniguchi, P. Moon, M. Koshino, P. Jarillo-Herrero, and R. C. Ashoori, *Science* **340**, 1427 (2013).
- [9] A. F. Young, J. D. Sanchez-Yamagishi, B. Hunt, S. H. Choi, K. Watanabe, T. Taniguchi, R. C. Ashoori, and P. Jarillo-Herrero, *Nature (London)* **505**, 528 (2014).
- [10] F. Amet, A. J. Bestwick, J. R. Williams, L. Balicas, K. Watanabe, T. Taniguchi, and D. Goldhaber-Gordon, *Nat. Commun.* **6**, 5838 (2015).
- [11] A. A. Zibrov, E. M. Spanton, H. Zhou, C. Kometter, T. Taniguchi, K. Watanabe, and A. F. Young, *Nat. Phys.* **14**, 930 (2018).
- [12] H. Polshyn, H. Zhou, E. M. Spanton, T. Taniguchi, K. Watanabe, and A. F. Young, *Phys. Rev. Lett.* **121**, 226801 (2018).
- [13] S. Chen, R. Ribeiro-Palau, K. Yang, K. Watanabe, T. Taniguchi, J. Hone, M. O. Goerbig, and C. R. Dean, *Phys. Rev. Lett.* **122**, 026802 (2019).
- [14] Y. Zeng, J. I. A. Li, S. A. Dietrich, O. M. Ghosh, K. Watanabe, T. Taniguchi, J. Hone, and C. R. Dean, *Phys. Rev. Lett.* **122**, 137701 (2019).
- [15] H. Zhou, H. Polshyn, T. Taniguchi, K. Watanabe, and A. F. Young, *Nat. Phys.* **16**, 154 (2020).
- [16] F. Yang, A. A. Zibrov, R. Bai, T. Taniguchi, K. Watanabe, M. P. Zaletel, and A. F. Young, *Phys. Rev. Lett.* **126**, 156802 (2021).
- [17] V. M. Apalkov and T. Chakraborty, *Phys. Rev. Lett.* **105**, 036801 (2010).
- [18] A. A. Zibrov, C. Kometter, H. Zhou, E. M. Spanton, T. Taniguchi, K. Watanabe, M. P. Zaletel, and A. F. Young, *Nature (London)* **549**, 360 (2017).
- [19] P. Maher, C. R. Dean, A. F. Young, T. Taniguchi, K. Watanabe, K. L. Shepard, J. Hone, and P. Kim, *Nat. Phys.* **9**, 154 (2013).
- [20] P. Maher, L. Wang, Y. Gao, C. Forsythe, T. Taniguchi, K. Watanabe, D. Abanin, Z. Papic, P. Cadden-Zimansky, J. Hone, P. Kim, and C. R. Dean, *Science* **345**, 61 (2014).
- [21] A. Kou, B. E. Feldman, A. J. Levin, B. I. Halperin, K. Watanabe, T. Taniguchi, and A. Yacoby, *Science* **345**, 55 (2014).
- [22] J. I. A. Li, C. Tan, S. Chen, Y. Zeng, T. Taniguchi, K. Watanabe, J. Hone, and C. R. Dean, *Science* **358**, 648 (2017).
- [23] F. Pientka, J. Waissman, P. Kim, and B. I. Halperin, *Phys. Rev. Lett.* **119**, 027601 (2017).
- [24] B. M. Hunt, J. I. A. Li, A. A. Zibrov, L. Wang, T. Taniguchi, K. Watanabe, J. Hone, C. R. Dean, M. Zaletel, R. C. Ashoori, and A. F. Young, *Nat. Commun.* **8**, 948 (2017).
- [25] H. Fu, K. Huang, K. Watanabe, T. Taniguchi, and J. Zhu, *Phys. Rev. X* **11**, 021012 (2021).
- [26] A. M. Seiler, F. R. Geisenhof, F. Winterer, K. Watanabe, T. Taniguchi, T. Xu, F. Zhang, and R. T. Wietz, *Nature (London)* **608**, 298 (2022).
- [27] K. Huang, H. Fu, D. R. Hickey, N. Alem, X. Lin, K. Watanabe, T. Taniguchi, and J. Zhu, *Phys. Rev. X* **12**, 031019 (2022).
- [28] R. B. Laughlin, *Phys. Rev. Lett.* **50**, 1395 (1983).
- [29] E. Y. Andrei, G. Deville, D. C. Glatli, F. I. B. Williams, E. Paris, and B. Etienne, *Phys. Rev. Lett.* **60**, 2765 (1988).
- [30] Z.-W. Zuo, A. C. Balram, S. Pu, J. Zhao, T. Jolicoeur, A. Wójs, and J. K. Jain, *Phys. Rev. B* **102**, 075307 (2020).
- [31] M. Shayegan, in *Les Houches 1998*, edited by A. Comtet, Th. Jolicoeur, S. Ouvry, and F. David, Topological Aspects of Low-Dimensional Systems (Springer, New York, 2000).

- [32] M. B. Santos, Y. W. Suen, M. Shayegan, Y. P. Li, L. W. Engel, and D. C. Tsui, *Phys. Rev. Lett.* **68**, 1188 (1992).
- [33] M. B. Santos, J. Jo, Y. W. Suen, L. W. Engel, and M. Shayegan, *Phys. Rev. B* **46**, 13639 (1992).
- [34] H. C. Manoharan, Y. W. Suen, M. B. Santos, and M. Shayegan, *Phys. Rev. Lett.* **77**, 1813 (1996).
- [35] M. K. Ma, K. A. Villegas Rosales, H. Deng, Y. J. Chung, L. N. Pfeiffer, K. W. West, K. W. Baldwin, R. Winckler, and M. Shayegan, *Phys. Rev. Lett.* **125**, 036601 (2020).
- [36] E. H. Rezayi, F. D. M. Haldane, and K. Yang, *Phys. Rev. Lett.* **83**, 1219 (1999).
- [37] F. D. M. Haldane, E. H. Rezayi, and K. Yang, *Phys. Rev. Lett.* **85**, 5396 (2000).
- [38] K. Yang, F. D. M. Haldane, and E. H. Rezayi, *Phys. Rev. B* **64**, 081301 (2001).
- [39] H. Wang, D. N. Sheng, L. Sheng, and F. D. M. Haldane, *Phys. Rev. Lett.* **100**, 116802 (2008).
- [40] E. McCann and V. I. Fal'ko, *Phys. Rev. Lett.* **96**, 086805 (2006).
- [41] K. Snizhko, V. Cheianov, and S. H. Simon, *Phys. Rev. B* **85**, 201415 (2012).
- [42] Z. Papić and D. A. Abanin, *Phys. Rev. Lett.* **112**, 046602 (2014).
- [43] T. Jolicoeur, C. Töke, and I. Sodemann, *Phys. Rev. B* **99**, 115139 (2019).
- [44] J. K. Jain, *Composite Fermions* (Cambridge University Press, Cambridge, 2007).
- [45] F. D. M. Haldane, in *The Quantum Hall Effect*, edited by R. E. Prange and S. M. Girvin (Springer, New York, 1987).
- [46] Z. Papić, D. A. Abanin, Y. Barlas, and R. N. Bhatt, *Phys. Rev. B* **84**, 241306 (2011).
- [47] Z. Zhu, D. N. Sheng, and I. Sodemann, *Phys. Rev. Lett.* **124**, 097604 (2020).
- [48] J. Zhao, Y. Zhang, and J. K. Jain, *Phys. Rev. Lett.* **121**, 116802 (2018).